Optimal Blurring and Illumination Patterns for Leukocytes Classification

Gianluca Di Muro
Department of Mechanical Engineering and Materials Science
Duke University
Durham, NC 27708
gianluca.dimuro@duke.edu

Abstract

This paper investigates optimal blurring and optimal incoherent illumination patterns, to correctly classify leukocytes. We simulate the physical layer, assuming a perfect incoherent light source, whose intensity is adjustable, for each color channel. Similarly we jointly learn an optimal blur, while training a Convolution Neural Network (CNN) to perform the classification task. Before entering the digital layer, the image is downsampled and converted to grayscale. A sensitivity analysis is performed varying the downsampling factor from 2 to 6 and is compared with a network fed with non-optimized physical layer, but without downsampling. Results show that physical layer optimization is able to completely offset a downsample factor of order of 3 and, even for lower resolutions, is still capable to provide a reasonable performance.

1 Introduction

Leukocytes classification may be crucial in identifying various diseases [10]. Among others, Acevedo *et al.* and have been applied deep learning for developing an automated system to correctly identify leukocytes in blood samples [1]. While their proposed methodology achieved overall good prediction performance, it requires high resolution imaging, resulting in high cost, specialized hardware and suffering of the resolution - field width dilemma, typical of microscopes.

In this project, we consider the same task investigated by the mention study, including a physical layer to simulate the light propagation, in order to jointly optimize the overall setup for achieving good performance, even when the input imaging are of lower quality. Figure 1 shows a schematic diagram of the simulation setup considered for this project. The common digital layer has been augmented with the image formation up to the sensor where the CNN is finally entered. This system adds further parameters, representing physical settings, which might be tuned on a practical apparatus in order to improve the model accuracy.

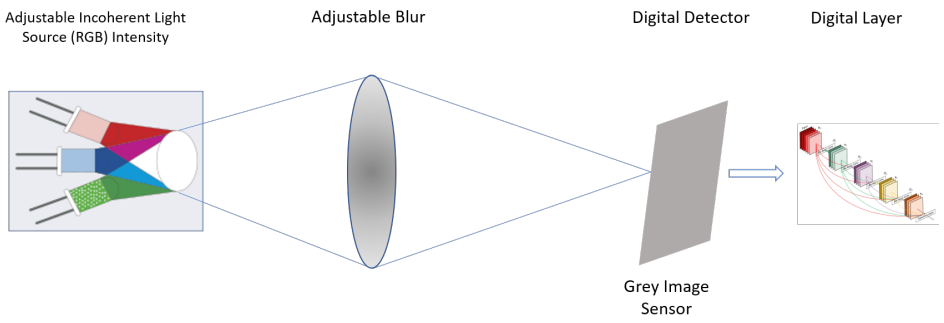

Figure 1: schematic diagram of the simulation setup.

2 Related work

CNNs have been successfully adopted for a plethora of applications and have been become increasingly popular with the advent of deep learning [7, 8]. Most recently a promising area of research has augmented the traditional CNN architectures with a physical layer, to include physical parameters pertaining the overall classification task in the optimization so to provide machine with the ideal setup for achieving better performance [3, 5, 9, 11]. We take inspiration from this novel approach, adopting a simplified version and applying this more inclusive optimization to the classification task tackled by Acevedo *et al.*. Specifically we want to investigate how physical parameters optimization may offset an increasing image resolution degradation.

3 Methods

3.1 Physical layer: incoherent lightning approximation

The physical layer simulates the image formation and its role is to closely represent the physical setup, so that physical parameters can be optimize in order to provide the digital layer with the best possible input image, for a given amount of information. We have assumed that we can adjust three LED diffused lights, so that the hypothesis of incoherent lightning is justified. Under these premises the imaging system is linear in intensity, when referred to the three channels [4].

Afterwards, the image is blurred through a pupil function provided by an aperture in the Fourier domain of unitary radius and multiplied with a matrix of adjustable weights: real and positive, to be consistent with the incoherent lightning hypothesis. Finally the image is formed on a monochromatic sensor, so the three channels are composed using a weighted average whose weights are to be optimized. We mention the fact that a bug in the code resulted in forming the gray image before the blur and then processing it through the blur. While this partially departs from the representative physical setup, we observe the degrees of freedom provided are still the same and that, even if the physical parameters are not promptly applicable, it is possible to find an equivalent physical setup: so the conclusions of this project remain valid.

In order to mimic a loss in resolution and to experiment whether it is possible to have an efficient classification with lower microscope magnification factors, the image is downsample through a average pooling layer, before being fed to the CNN.

3.2 Digital layer: DenseNet-121

The digital layer is comprised of a DenseNet-121 [6]. This architecture has been chosen to avoid the zero gradient problem and for sufficiently expected high performance, while keeping the number of weights limited. The input layer of the network has been automatically adapted to the incoming data, depending on the resolution of the sample, which is a function of the pooling size chosen for the specific numerical experiment. The top and final layer of the network has been substituted with a dense layer, piping into a softmax layer, so that the output of the network can be easily interpreted as predicted probabilities of each individual class.

4 Results

4.1 Data Description

We have used high quality annotated data, published in [2]. Original stained blood samples have been collected and annotated, offering a versatile tool to experiment with supervised learning algorithms. Leukocytes have been divided in eight classes, namely: basophil, eosinophil, immature granulocytes, lymphocyte, monocyte, neutrophil, platelet, and erythroblast, shown in figure 2. As it is evident we do not consider the erythroblast class in this study, because we had problems in loading the data from the relevant source: so, for our analyses we will deal with only the first seven categories; nevertheless, the final layer of all the networks is comprised of eight units, to be applicable to the complete dataset. We briefly mention that, consistently with the training data, no input has been assigned to the erythroblast category, neither in the training nor in the validation datasets.

All images have a consistent resolution of 363×360 pixels, in format JPG and present three color channels.

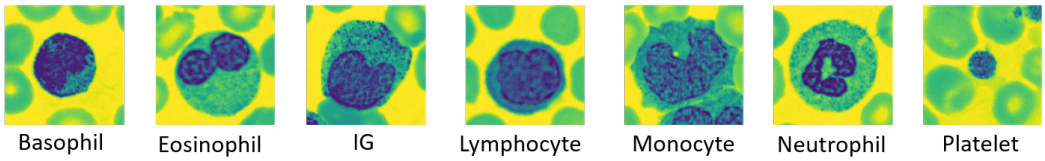

Figure 2: classes of leukocytes with relevant images.

4.2 Simulation setup and findings

The original data have been cropped to a resolution of 200×200 pixels, then have been augmented, using rotation of up to 25° and being flipped horizontally and vertically.

Five CNNs have been successfully trained, with increasing value of pooling size for the average pooling layer, ranging from one to six. We used the only CNN without loss of the input resolution as a benchmark, to see how the classification accuracy would deteriorate, dealing with increasing lower information. On converse, to emphasize the expected beneficial effects provided by the physical layer, we have frozen the physical parameters for this network, so to contrast higher information in the fed images with *ad hoc* set up flexibility provided by the physical layer optimization. We refer to these networks as NoOpt1, Opt2, Opt4, Opt5, and Op6, respectively.

For all the five networks the Adam optimizer has been adopted, experimenting with different learning rates, all the range of $(10^{-4}, 10^{-3})$ and the training has been protracted until a new maximum had not been seen for at least 10 epochs, in the validation set. All the reported results refer to the validation performance. Finally a cross entropy categorical loss function has been adopted, since we consider a multi classification problem.

Table 1 shows the overall validation accuracy for all the considered models. Unexpectedly Op2 performed worse than Opt4 and even than Opt5, this most likely suggests that it is a sub-optimal solution and training should be performed again, possibly with a different learning rates and with a different weight initialization.

Table 1: Overall validation accuracy

Network Name	Optimized Physical Layer	Downsample Factor	Accuracy (%)
NoOpt1	No	1	96.08
Opt2	Yes	2	93.60
Opt4	Yes	4	95.75
Opt5	Yes	5	94.18
Opt6	Yes	6	92.86

Figure 3 shows a training and validation accuracy, as a function of the epochs. Overall overfitting does not seem to be significant, since the validation accuracy follows reasonably well the training accuracy. The training has been halted, mainly for the reason of avoiding overfitting, since the validation loss had not been improving for ten epochs, as described.

Figure 3: representative training, for Opt4.

Figure 4 show the confusion matrices, with increasing value for the downsample parameter. The general performance of the classification task is comparable and in agreement with the one reported in [1]. For example, with their best network, the Authors achieve an overall performance of 96%, which is equal to the performance of NoOpt1. A couple of observfations: Opt4, taking advantage of the physical layer optimization, gets a similar performance of 95.75%, while being fed with an image with $\frac{1}{16}$ of the pixels. On converse, it is worth recalling the fact that our data have only seven categories of the original eight: so we should retest our current simulation on the complete dataset, for a fairer comparison.

We conclude the results analysis, showing the learned optimal blur and the output of the physical layer, for assessing the effect of the physical setup on the overall classification performance; moreover, it is interesting to analyze to see whether some apparent patterns appear.

Figure 5 shows the learned optimal blur, for Opt6. It is apparent a circular symmetry with the highest value of the matrix achieved at the center and along a circular crown.

Figure 6 shows the effect of the physical layer on the various classes. We decided to present the results for Opt6 because is the most aggressive downsample case, so the physical layer has to make up for the biggest loss of information among the cases analyzed: so we speculate that any pattern might be more evident in this case. In all the presented images, as well as in most of the others examined and not presented here, seem to present a quite clear aura around the contour of the leukocyte which, most likely, helps the subsequent digital layers in achieving better classification performance, albeit with scarser information.

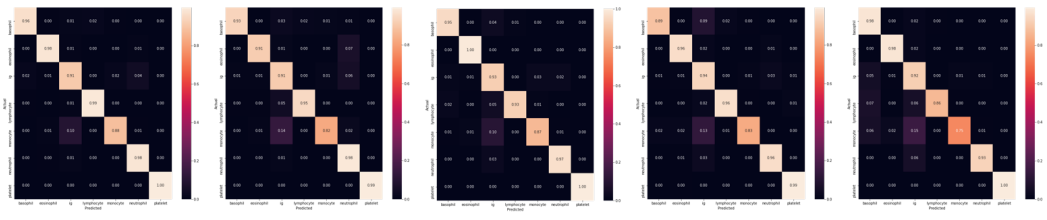

Figure 4: classes of leukocytes with relevant images.

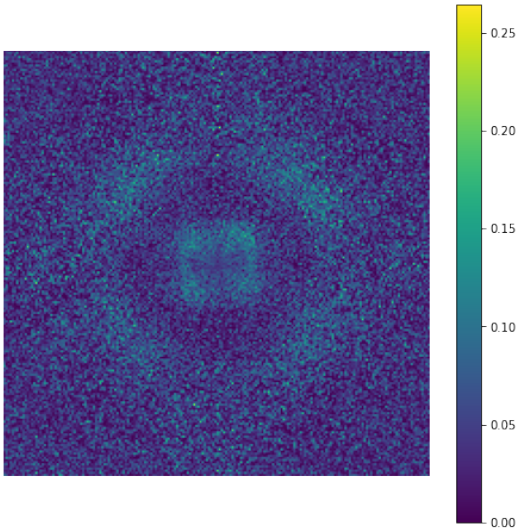

Figure 5: learned optimal blur, for Opt6.

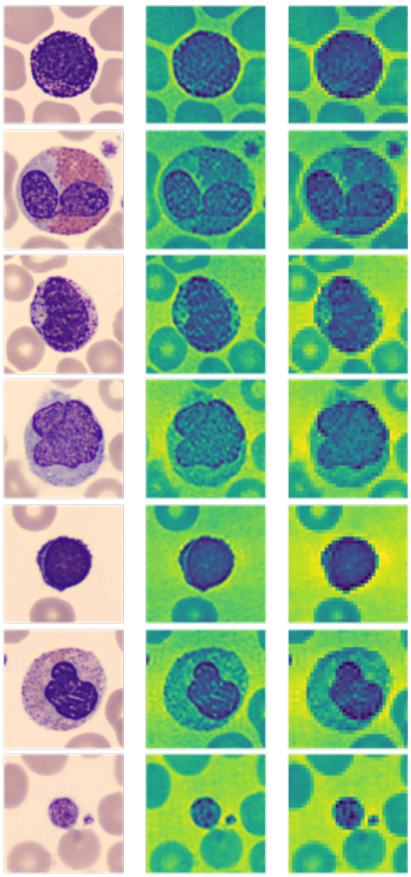

Figure 6: from left to right: original input, output from the physical layer before the downsampling, actual input to the digital layer, for Opt6.

5 Discussion

This project successfully showed how physical layers may be pivotal in finding optimal setup for automatic classification. Classification performance was still very good even after image deterioration through down sampling: this could be potentially useful leading to adopt a cheaper apparatus and also allowing clinical pathologist to adopt lower magnifications.

Future work may consider more complex setups, where further physical parameters may be learned, jointly with the network parameters; also one could conduct further numerical experiments, considering other CNNs architecture and broadening the choice of hyperparameters in order to aim for higher classification performance.

References

[1] A. Acevedo, S. Alférez, A. Merino, L. Puigví and J. Rodellar, "Recognition of peripheral blood cell images using convolutional neural networks" Computer Methods and Programs in Biomedicine, 180:105020 (2019).

[2] A. Acevedo, A. Merino, S. Alférez, A. Molina, L. Boldú, J. Rodellar, "A dataset for microscopic peripheral blood cell images for development of automatic recognition systems", Mendeley Data, VI, doi: 10.17632/snkd93bnjr.1 (2020).

[3] C. Cooke, F. Kong, A. Chaware, K. Zhou, K. Kim, R. Xu, D. M. Ando, S. J. Yang, P. C. Konda and R. Horstmeyer, "Physics-enhanced machine learning for virtual fluorescence microscopy", arXiv: 2004.04306vs (2020).

[4] J. W. Goodman, "Introduction to Fourier Optics", 2nd ed., The McGraw-Hill Companies (1996).

[5] R. Horstmeyer, R. Chen, B. Kappes, B. Judkewitz, "Convolutional neural networks that teach microscopes how to image", arXiv: 1908.00620, (2019).

[6] G. Huang, Z. Liu, L. Van Der Maaten and K. Q. Weinberger, ""Densely Connected Convolutional Networks", 2017 IEEE Conference on Computer Vision and Pattern Recognition (CVPR), Honolulu, HI, pp. 2261-2269 (2017).

[7] Y. LeCun, Bottou and Y Bengio, "Gradient-based learning applied to document recognition" Proceedings of the IEEE, 2278-2324 (1998).

[8] Y. LeCun, Y. Bengio and G. Hinton, "Deep Learning" Nature 521 , 436–444 (2015).

[9] A. Muthumbi, A. Chaware, K. Kim, K. C. Zhou, P. C. Konda, R. Chen, B. Judkewitz, A. Erdmann, B. Kappes and Roarke Horstmeyer, "Learned sensing: jointly optimized microscope hardware for accurate image classification" Biomed. Opt. Express, 10(12):6351-6369, (2019).

[10] M. Saraswat and K. V. Aray, "Automated microscopic image analysis for leukocytes identification: A survey" Micron, 65:20-33 (2014).

[11] G. Zheng, R. Horstmeyer and C. Yang, "Wide-field, high-resolution Fourier ptychographic microscopy" Nature Photonics 7, 739-745 (2013).